J. Fluid Mech. (1994), *vol.* 280, *pp.* 335–347

A stationary potential-flow approximation for a breaking-wave crest

By ALASTAIR D. JENKINS†

The IBM Environmental Sciences and Solutions Centre, Bergen, Norway

(Received 23 August 1993 and in revised form 4 July 1994)

The flow in a breaking-wave crest is represented by a complex velocity potential on a Riemann surface, satisfying the Bernoulli condition on two free boundaries. The flow is assumed to be stationary in the reference frame which moves with the wave crest, and at large distances approximates Stokes corner flow in the main part of the fluid and a parabolic descending flow in the jet. The interaction of the jet with the rest of the fluid is neglected.

The solution is obtained by means of a conformal transformation from a bounded, teardrop-shaped domain, using a Faber polynomial expansion. The Bernoulli condition is applied at a number of discrete points on the boundaries, and the resulting nonlinear equations for the expansion coefficients are solved iteratively. The resulting surface form is similar to that obtained by laboratory experiments and time-dependent numerical simulations of waves up to the point of breaking, with a stagnation point at the top of the crest, an overturning loop with major axis $\approx 8g^{-\frac{1}{3}}\Psi^{\frac{2}{3}}$, and a maximum acceleration of $\approx 5.4g$, where g is the gravitational acceleration and Ψ is the flux in the jet.

1. Introduction

The present study was prompted by the observation that the form of the free surface in the crests of irrotational surface gravity waves on an incompressible fluid, at the point of breaking, appears to be very similar for many laboratory experiments (Miller 1957; Vinje & Brevig 1981; Dommermuth *et al.* 1988; Bonmarin 1989) and time-dependent numerical simulations (Longuet-Higgins & Cokelet 1976; Dold & Peregrine 1984; New, McIver & Peregrine 1985; Dommermuth *et al.* 1988; Seo & Dalrymple 1990; Dold 1992). This suggests that there is a basic similarity in the flow, which might be reproduced using a relatively simple approximation, and indeed a number of theoretical studies have produced simple analytical time-dependent descriptions of various parts of the flow in irrotational breaking waves (Longuet-Higgins 1976, 1980*a*,*b*, 1981, 1982, 1983; Greenhow 1983; New 1983).

However, an alternative approach, used in the present paper, is to see whether the flow in a breaker can be approximated by a stationary flow pattern. An indication that this might be useful is given by the fluid particle accelerations shown in figure 6(*b*) of Dommermuth *et al.* (1988), which, in the overturning loop on the underside of the jet, are directed approximately towards the centre of curvature of the surface, having magnitudes several times the gravitational acceleration g. This suggests that in

† Present address: Nansen Environmental and Remote Sensing Center, Edvard Griegs vei 3a, N–5037 Solheimsviken, Bergen, Norway

this region the free surface lies approximately along a streamline, so that a steady-flow approximation could be valid.

Of course, if the flow is steady, the jet of the breaker will intersect the forward face of the wave, so that the complex velocity potential χ will be defined on a Riemann surface which is different from a simple complex plane. In reality, the jet will mix turbulently with the rest of the fluid and air bubbles will be entrained, but it may be possible to treat these effects separately (e.g. Hwang, Poon & Wu 1991), and regard them as contributions to a 'weak-in-the-mean' process (Hasselmann 1974) which has just a small effect on the fluid motion elsewhere. The momentum of the fluid in the jet will be dissipated, so it will contribute to the loss of momentum from the wave field, and hence to the loss of wave energy. In this way an irrotational breaking crest will provide a contribution to wave energy dissipation which can be calculated 'from first principles' (cf. Jenkins 1994).

Dias & Tuck (1993) computed such a breaking-wave flow pattern for a hydraulic jump in shallow water, commenting that the jet was assumed to fall 'as if into a bottomless chasm'. Dias & Christodoulides (1991) computed a similar type of flow which represents a ship's breaking bow wave.

In §2.1 I present a potential flow which has the same topology as the flow in a breaking-wave crest of stationary form, has similar asymptotic behaviour at large distances, and satisfies the free-surface Bernoulli condition on a single streamline. This is then modified numerically in §2.2, to satisfy the Bernoulli condition on both free surfaces, the other surface containing a stagnation point. A numerical solution is presented in §2.3, and a discussion of the behaviour of the flow in the far field and the uniqueness of the flow is presented in §§2.4–2.5.

Though most breaking waves in the open ocean can be regarded as 'spilling breakers', and do not have the characteristic shape of a plunging breaker, shown in this paper, in time-dependent simulations, and in laboratory experiments, they can probably be regarded as being basically the same phenomenon except with a smaller length scale. The structure of the 'irrotational' part of the crest then becomes hidden by chaotic and turbulent motions, surface foam and sea spray.

2. Quasi-stationary solution

If a breaking-wave crest can be approximated by a stationary pattern of potential flow, we can think of such a pattern as approximating two different simpler flows at large distances, in different parts of the Riemann surface which represents the spatial coordinates (Re z, Im z). In the main part of the fluid it will approximate Stokes corner flow, as in the case of the crest of an 'almost-highest wave' (Longuet-Higgins & Fox 1977). In the jet protruding from the crest it should approximate a flow in which the fluid particles are in free fall and execute parabolic trajectories. Various authors have published analytical and numerical treatments of two-dimensional potential flow in jets with free surfaces, influenced by gravity, and related phenomena (e.g. Bervi 1894; Birkhoff & Carter 1956; Birkhoff & Zarantonello 1957; Clarke 1965; Gurevich 1966; Keller & Geer 1973; Ting & Keller 1974; Geer & Keller 1979; Vanden-Broeck & Keller 1982, 1986; Goh & Tuck 1985; Tuck 1987; Dias, Keller & Vanden-Broeck 1988; Feng 1988; Dias & Christodoulides 1991; Dias & Tuck 1993; Lee & Vanden-Broeck 1993). The present treatment is similar to that of Longuet-Higgins & Fox (1977), but the free-surface boundary conditions are applied at discrete points, as in Birkhoff & Carter (1956, appendix D), Birkhoff & Zarantonello (1957), Vanden-Broeck & Keller

(1986, 1989), Dias *et al.* (1988), Dias & Christodoulides (1991), Dias & Tuck (1993) and Lee & Vanden-Broeck (1993).

We let the real z-axis point vertically upwards and the imaginary axis point to the left, with the wave travel direction towards the right. Since we have steady, two-dimensional potential flow, the free surfaces are streamlines and the fluid velocity is given by the complex conjugate of the derivative of the velocity potential χ:

$$v = (\mathrm{d}\chi/\mathrm{d}z)^*. \tag{2.1}$$

On the free-surface streamlines we have the constant-pressure Bernoulli condition

$$\tfrac{1}{2}|v|^2 + \mathrm{Re}\, z = \text{const.}, \tag{2.2}$$

where we choose length units so that $g = 1$.

2.1. *An exact solution*

The following complex velocity potential satisfies exactly the boundary condition (2.2) at a free surface which follows the streamline $\mathrm{Im}\, \chi = 0$:

$$\chi = -\tfrac{2}{3}\mathrm{i} + 2\mathrm{i}(z+2) - \tfrac{1}{3}\mathrm{i}(2(z+2))^{3/2}. \tag{2.3}$$

Part of the flow, which has the same topology as flow in a breaking wave crest, is shown in figure 1. The free-surface streamline $\mathrm{Im}\, \chi = 0$, which is a parabola, is labelled AA'. The fluid occupies the region above this streamline (including the part above the line BSB', where the streamlines have been omitted), where there are no singularities in χ. Below AA' there is a branch point singularity at $z = -2$. This flow can be derived by analytic continuation of a velocity potential which describes the flow along AA' in which fluid particles are in free fall under the influence of gravity, with velocity component -1 in the $\mathrm{Im}\, z$ direction, (cf. John 1953).

The streamline $\mathrm{Im}\, \chi = \Psi = \frac{2}{3}$ has a stagnation point S at $z = 0$, where $\mathrm{Re}\, \chi = 0$. This streamline then splits into two parts, SB and SB'. Although the Bernoulli condition is not satisfied on BSB', we describe in §§2.2–2.4 a modified flow pattern which does satisfy it on both surfaces. The surface SB then corresponds to the rear part of a wave crest and SB' to the upper surface of the jet, the flux in the jet being $\Psi = \frac{2}{3}$. The leading-order asymptotic behaviour of (2.3), $\chi \sim (\text{const.})z^{3/2}$ as $|z| \to \infty$, is the same as for Stokes corner flow except for the orientation and the constant of proportionality (Longuet-Higgins 1981).

Flows of the form (2.3) with $\Psi \neq \frac{2}{3}$, still satisfying (2.2) on $\mathrm{Im}\, \chi = 0$, may be obtained by multiplying χ by $\frac{3}{2}\Psi$, and the horizontal and vertical length scales by $(\frac{3}{2}\Psi)^{2/3}$, whereby the velocities are all multiplied by $(\frac{3}{2}\Psi)^{1/3}$.

2.2. *Modification of the flow*

Equation (2.3) can be inverted, using the cubic equation formula, so that z can be expressed as a function of χ. Care must be taken to choose the correct branch of the solution. In order to modify the flow (2.3) so that it satisfies (2.2) on both free surfaces, we displace z and multiply it by a polynomial series in a new complex variable Ω. We call the new complex spatial variable Z, and we have

$$Z - Z_0 = (z - z_0)h(\Omega); \qquad h(\Omega) = \sum_{j=0}^{\infty} w_j\, p_j(\Omega); \tag{2.4}$$

where the relation between z and Ω is given by (2.3), together with

$$\chi = \tfrac{1}{3}\mathrm{i} + \tfrac{2}{3}\pi^{-1}(-1 - b + b_0 + \mathrm{i}\mathrm{e}^{b-b_0}), \tag{2.5a}$$

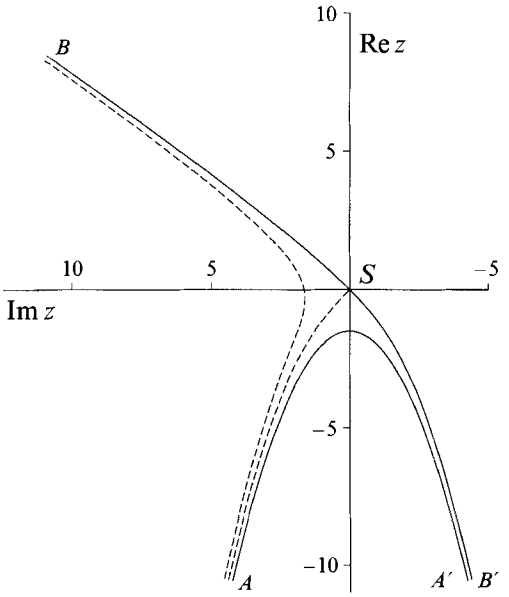

FIGURE 1. A flow which satisfies the free-surface boundary condition on streamline AA'. Solid lines represent free surfaces of the wave crest (Im $\chi = 0, \frac{2}{3}$); broken lines represent interior streamlines (Im $\chi = \frac{2}{3}, \frac{4}{3}$).

$$b = \pi a - \log(\tfrac{1}{2}(1 - e^{\pi a})), \tag{2.5b}$$

and

$$a = \tan(\tfrac{1}{4}\pi(\Omega - 1)). \tag{2.5c}$$

Note that the relation between z and χ is kept fixed, being given by (2.3). In the complex b-plane, the fluid occupies the strip $|\text{Im } b| \leqslant \frac{1}{2}\pi$, with the stagnation point at $b = b_0 - \frac{1}{2}i\pi$. The constants b_0 and z_0 can be adjusted as required, and Z_0 is determined by the condition that the stagnation point S is at $Z = 0$. Figure 2 shows streamlines in the complex Ω-plane for $b_0 = -4.5$. The fluid fills the teardrop-shaped domain T, and the free surfaces follow its boundary ∂T. The $p_j(\Omega)$ in (2.4) are Faber polynomials, as defined in §18.2 of Henrici (1986), and can be evaluated from the coefficients of the Laurent series expansion of the conformal mapping $\Omega = \gamma(\omega)$ of the exterior of the unit circle

$$\omega = e^{i\theta}, \qquad \theta \in (-\pi, \pi], \tag{2.6}$$

onto the exterior (complement) of T. Faber polynomials provide a way of constructing uniformly convergent series approximations for functions defined in simply connected, compact domains in the complex plane, in a similar way to the construction of Taylor series approximations for functions in circular domains.

According to theorem 18.2a of Henrici (1986), the series $\sum_0^\infty w_j p_j(\Omega)$ is uniformly convergent in T if h is analytic in an open set containing T. Since the boundary ∂T of T is a Jordan curve with bounded rotation and its only corner has an exterior angle (at $\Omega = -1$) which is non-zero, Henrici's lemma 18.2d implies that the $p_j(\Omega)$ are bounded within T and on ∂T, as $j \to \infty$. Also, the coefficients w_j are equal to the corresponding Fourier coefficients with respect to θ of $h(\gamma(e^{i\theta}))$. The Faber polynomial expansion can then be extended to include functions h which are analytic

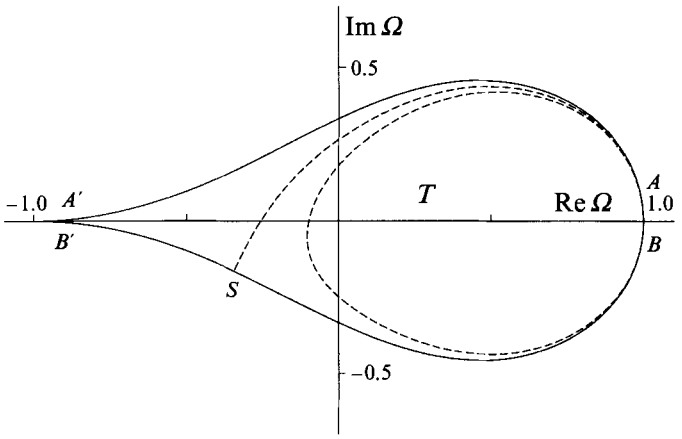

FIGURE 2. Flow in the Ω-plane. The teardrop-shaped domain T is filled with fluid, and the streamlines with Im $\chi = 0$, $\frac{2}{3}$, and $\frac{4}{3}$ are shown.

in the interior of T and have absolutely convergent Fourier series for $h(\gamma(e^{i\theta}))$ on $\gamma(e^{i\theta}) \in \partial T$. In §2.4 I show that this is the case for $h = (Z - Z_0)/(z - z_0)$ in the current problem.

The series (2.4) thus converges in the interior of T and on its boundary ∂T, in a similar way to the convergence inside and on the circle $|\omega| = 1$ of the power series of Longuet-Higgins & Fox (1977, equation 6.4). It is necessary to use a teardrop-shaped domain rather than a circle, because for a circular domain the mapping of the flow in the region of the jet has logarithmic behaviour and the convergence is unacceptably slow. The required conformal mapping was computed numerically using the fast Fourier transform method of Wegmann (1978), as described by Henrici (1986, §16.9). Note that there are some errors in Henrici's presentation, in the first three equations on p. 418, and in the formula for $\lambda(s)$ on p. 422. Since Wegmann's method is directly applicable only to domains with smooth boundaries, it was applied for the mapping from the exterior of the unit circle to the exterior of a smooth curve in the plane of another complex variable Ξ. This curve becomes the boundary ∂T of T in the Ω-plane under the Joukowski map

$$\Omega = \tfrac{3}{8}(\Xi + \Xi^{-1}) - \tfrac{1}{4}. \tag{2.7}$$

To obtain good convergence with Wegmann's method, it was necessary to use a large number of points on the boundary: the computations reported in this paper used 2048 points.

The expansion (2.4) is substituted into the free-surface Bernoulli condition written in the following form:

$$|\Omega - \Omega_0|^2 \left((Z + Z^*) \frac{\mathrm{d}Z}{\mathrm{d}\chi} \left(\frac{\mathrm{d}Z}{\mathrm{d}\chi} \right)^* + 1 \right) = 0, \tag{2.8}$$

where Ω_0 is the value of Ω at the stagnation point S. The factor $|\Omega - \Omega_0|^2$ is applied in order to counteract the singularity of $(\mathrm{d}Z/\mathrm{d}\chi)(\mathrm{d}Z/\mathrm{d}\chi)^*$ at S. Condition (2.8) is applied at a number of discrete collocation points Ω_j on ∂T. The points are an evenly distributed subset of those used in Wegmann's method for the exterior conformal mapping. They become equally spaced if we map the exterior of T onto

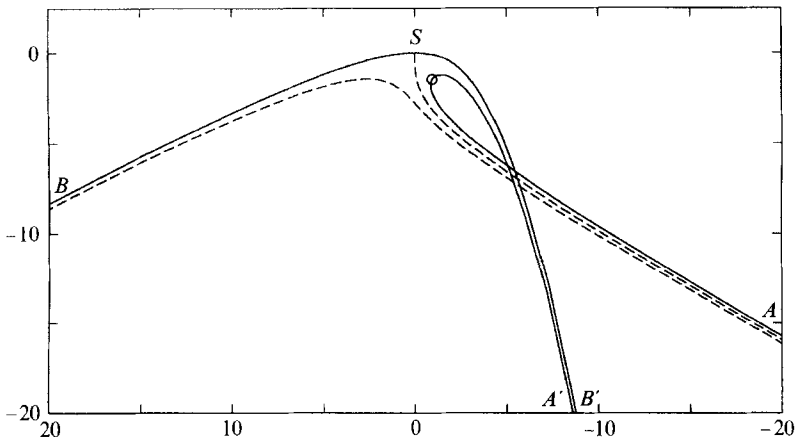

FIGURE 3. Flow which represents a breaking-wave crest of constant form. It satisfies the free-surface boundary condition at 128 points on the surface. The circle marks the position of maximum fluid acceleration ($\approx 5.4g$). The length scale is adjusted so that the flux through the jet and the intervals between the streamlines shown have unit magnitude; using dimensional variables, the length unit is $L = g^{-1/3}\Psi^{2/3}$, where Ψ is the flux through the jet.

the exterior of the circle (2.6). The collocation points extend well out into the jet region near $\Omega = -1$: this would not be the case if a circular domain were used, with a logarithmic mapping of the flow in the jet region, as in Birkhoff & Carter (1956), Birkhoff & Zarantonello (1957), Vanden-Broeck & Keller (1986), Dias *et al.* (1988), Dias & Christodoulides (1991), Dias & Tuck (1993), and Lee & Vanden-Broeck (1993). For $2n$ points along the boundary, we obtain $2n$ nonlinear equations in $2n$ unknowns if we use Faber polynomials $p_0 \dots p_{n-1}$, the unknowns being the real and imaginary parts of the complex coefficients $w_0 \dots w_{n-1}$. The equations were solved using the subroutine C05PBF of NAG (1990), which employs an iterative technique – a modification of the Powell hybrid method.

2.3. *Solution for the flow*

With $z_0 = 3.5$, $b_0 = -4.5$, and 128 solution points, we obtain the flow shown in figure 3. The scaling relation between the length and velocity scales and the flux in the jet Ψ, described at the end of §2.1, applies to this flow, and the length scale has been changed so that the non-dimensional flux of fluid in the jet has magnitude 1 instead of $\frac{2}{3}$. In dimensional variables, the length unit is equal to $L = g^{-1/3}\Psi^{2/3}$. The fluid has maximum acceleration of approximately $5.4g$ on the underside of the crest, at the point marked with the circle.

Where the jet intersects the forward surface of the wave, the fluid velocity is $\approx 3.6V$, where $V = (g\Psi)^{1/3}$, and the horizontal component of the jet velocity is $\approx 1.2V$. The relative speed of the fluid in the jet with respect to the fluid at the front wave surface is $\approx 6.9V$.

The free surface is oriented horizontally at the stagnation point S, which is thus at the maximum height the fluid reaches. The free surface must be horizontal at S, since $|v|^2 \sim (\text{const.})|Z|^2$ as $|Z| \to 0$ if we locate S at $Z = 0$, from which the Bernoulli condition requires that $\text{Re}\, Z \sim (\text{const.})|Z|^2$ on the surface.

If varying values of the adjustable parameters (number of points, b_0, z_0) are used, the geometrical dimensions of the resulting numerically calculated flow vary by about

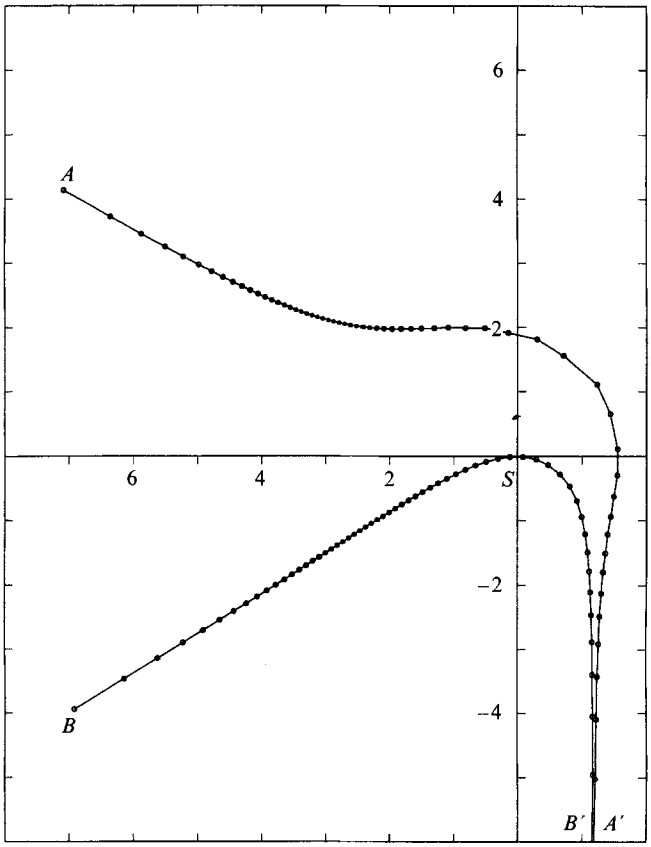

FIGURE 4. Hodograph of the velocity at the free surface, for the flow of figure 3. The circles mark the computed values. The surface AA' corresponds to the forward face of the wave and the underside of the jet, SB to the rear face of the wave and SB' to the upper surface of the jet. The units of velocity are $(g\Psi)^{1/3}$.

$\pm 5\%$. Bearing in mind that the assumption that the flow is stationary and irrotational is a radical simplification of the physical situation, this inaccuracy is acceptable. The inaccuracy may be due to somewhat poor convergence of the polynomial expansion: in §2.4 it is shown that the behaviour of $h = (Z - Z_0)/(z - z_0)$ as $|z| \to \infty$ is such that the polynomial series for $\mathrm{d}h/\mathrm{d}\Omega$, which is used in computing the surface boundary condition (2.8), is not convergent on ∂T, although its behaviour appears to be acceptable for small to moderately large values of $|z|$.

The velocity at the free surface in the flow of figure 3 is shown in hodograph form in figure 4. The velocity values obtained by direct application of (2.1) had some saw-toothed oscillations, probably due to the divergence of the polynomial series for $\mathrm{d}h/\mathrm{d}\Omega$. The amplitude of these oscillations was reduced by applying a three-point smoothing formula and then scaling the result so that it still satisfied the Bernoulli condition, so we obtain the following formula for smoothed velocities $\hat{v}_j$ from the computed positions Z_j and velocities v_j:

$$\hat{v}_j = (-2\mathrm{Re}\, Z_j)^{1/2} \frac{v_{j-1} + 2v_j + v_{j+1}}{|v_{j-1} + 2v_j + v_{j+1}|}. \tag{2.9}$$

In the jet region, the velocity converges to a vertical asymptote, indicating that the

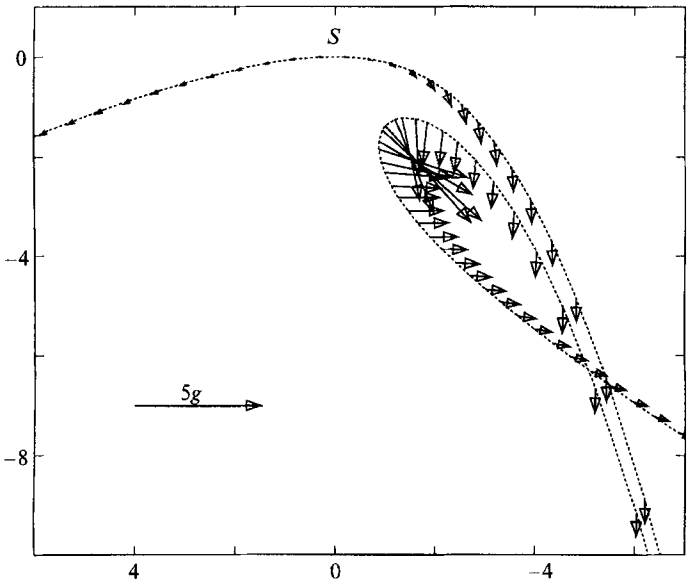

FIGURE 5. Accelerations at the free surface, for the flow of figure 3. The tails of the arrows are at the computed positions.

flow tends towards free fall under gravity. On the forward and rear faces of the wave, the velocity converges to asymptotes with slopes of $\pm 30°$, as in Stokes corner flow. These asymptotes do not actually go through the origin, so that the direction of the acceleration vector converges more rapidly to its Stokes corner flow value than the velocity vector does. The zero velocity, in the current frame of reference, at the stagnation point S, becomes a horizontal velocity equal to the phase velocity of the wave in an absolute frame of reference. This is confirmed in laboratory measurements of breaking waves by Sawada & Tomita (1994), which show large, horizontally directed velocity vectors in the region near the top of the crest.

Figure 5 shows the acceleration at the free surface near the wave crest. The saw-toothed behaviour of the acceleration computed directly from the polynomial expansion was unacceptably great, so smoothed values $\widehat{A}_j$ were calculated using finite differences:

$$\widehat{A}_j = \tfrac{1}{4}\left((\widehat{v}_{j+2} - \widehat{v}_{j-2}) + 2(\widehat{v}_{j+1} - \widehat{v}_{j-1})\right) \frac{|\widehat{v}_j| \operatorname{sign}(\chi_{j+2} - \chi_{j-2})}{|(Z_{j+2} - Z_{j-2}) + 2(Z_{j+1} - Z_{j-1})|}. \tag{2.10}$$

(Note that the expression is valid when $(\chi_{j+2} - \chi_{j-2})$ is real, i.e. when the points $(Z_{j-2}, \ldots Z_{j+2})$ are all on the same surface and all lie on the same side of the stagnation point S.)

In the jet, the acceleration tends toward the value $1.0\,g$, directed vertically downwards. The greatest accelerations are near the top of the loop on the underside of the crest, the maximum magnitude being $\approx 5.4\,g$.

2.4. *Behaviour of the flow in the far field*

Figure 6 shows the behaviour of the flow at large distances from the crest. The forward and rear faces of the wave can be seen to converge quite well to straight lines inclined at $\pm 30°$ to the horizontal, except for the two outermost computed points. This is in spite of the fact that the corresponding streamlines in the flow of

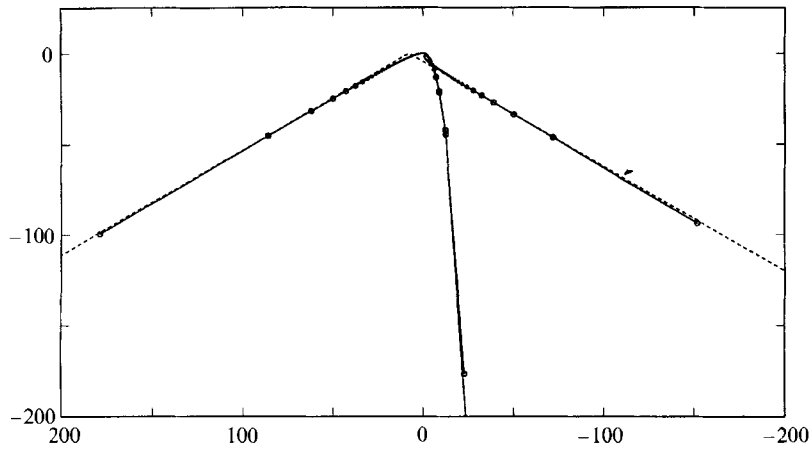

FIGURE 6. Behaviour at large distances, for the flow of figure 3. The circles show the computed positions, and are reduced in size where they are close together, so that they do not overlap. The broken lines, put in for comparison, have slopes of $\pm 30°$.

figure 1 are not asymptotic to straight lines, the surface AA' being a parabola. Hence the numerical solution for the function $h(\Omega)$ in (2.4) provides a reasonably good correction to the shape of the surface streamlines. The departure of the outermost two points from the asymptotes reflects the singularity of $h(\Omega)$ at $\Omega = 1$.

For Stokes corner flow we have $Z = -(-\frac{3}{2}\mathrm{i}\chi)^{2/3}$. In the present case, however, the presence of the jet requires us to have a source of fluid at infinity. To determine the behaviour of the flow in the far field we thus need to consider flows of the form

$$Z = -\left[-\tfrac{3}{2}\mathrm{i}(\chi - \tfrac{2}{3}\mathrm{i} + \tfrac{2}{3}\pi^{-1}\log\chi + \kappa(\chi))\right]^{2/3}, \tag{2.11}$$

where κ is a correction, becoming small with regard to the other terms as $|\chi| \to \infty$, which enables (2.11) to satisfy the Bernoulli condition on the free surface. Note that if $\kappa \to 0$, the free surfaces ($\chi = \phi + 0.\mathrm{i}$, $\phi \to -\infty$) and ($\chi = \phi + \frac{2}{3}\mathrm{i}$, $\phi \to +\infty$) become asymptotic to straight lines which pass through $Z = 0$ and are inclined at $\mp 30°$ to the horizontal.

The Bernoulli condition $(Z + Z^*)(\mathrm{d}Z/\mathrm{d}\chi)(\mathrm{d}Z/\mathrm{d}\chi)^* + 1 = 0$ implies that

$$-\left[\left(-\tfrac{3}{2}\mathrm{i}(\chi - \tfrac{2}{3}\mathrm{i} + \tfrac{2}{3}\pi^{-1}\log\chi + \kappa)\right)^{1/3}\left(\tfrac{3}{2}\mathrm{i}(\chi^* + \tfrac{2}{3}\mathrm{i} + \tfrac{2}{3}\pi^{-1}\log\chi^* + \kappa^*)\right)^{-1/3} + \text{c.c.}\right]$$
$$\times\left(1 + \tfrac{2}{3}\pi^{-1}\chi^{-1} + \frac{\mathrm{d}\kappa}{\mathrm{d}\chi}\right)\left(\cdots\right)^* + 1 = 0 \tag{2.12}$$

on the free-surface streamlines, where 'c.c.' represents the complex conjugate of the previous term and $(\cdots)^*$ represents the complex conjugate of the previous factor in parentheses.

We now introduce a new variable

$$\tau = \left(\chi - \tfrac{2}{3}\mathrm{i} + \tfrac{2}{3}\pi^{-1}\log\chi\right)^{-1}, \tag{2.13}$$

which tends to zero as $|\chi| \to \infty$. In the neighbourhood of $\tau = 0$, the fluid occupies the lower half-plane, and the free surface approximates the real τ-axis. The free-surface condition can then be written as

$$-\left[\left(-\tfrac{3}{2}\mathrm{i}(\tau^{-1}+\kappa)\right)^{1/3}\left(\tfrac{3}{2}\mathrm{i}(\tau^{*-1}+\kappa^{*})\right)^{-1/3}+\text{c.c.}\right]$$
$$\times\left(1+\tfrac{2}{3}\pi^{-1}\tau+\text{h.o.t.}-\frac{\mathrm{d}\kappa}{\mathrm{d}\tau}\left(\tau^{-2}+\text{h.o.t.}\right)\right)\left(\cdots\right)^{*}+1=0 \quad (\mathrm{Im}\,\tau=0), \tag{2.14}$$

where 'h.o.t.' means 'higher-order terms'.

Expanding (2.14) and neglecting terms of higher order than τ, we find that

$$\tau^{-2}\frac{\mathrm{d}}{\mathrm{d}\tau}(\mathrm{Re}\,\kappa)-\tfrac{1}{3}\tau\,\mathrm{Re}\,\kappa=\tfrac{2}{3}\pi^{-1}\tau \tag{2.15}$$

on the real τ-axis. This has solutions of the form

$$\kappa=(\text{const.})\exp\left(\tfrac{1}{12}\tau^{4}\right)-2\pi^{-1},$$

so $\kappa=O(1)$ in the neighbourhood of $\tau=0$; hence the free-surface streamlines are asymptotic to straight lines inclined at $\pm30°$ to the horizontal, and we can write

$$Z=-\left(-\tfrac{3}{2}\mathrm{i}\chi\right)^{2/3}\left(1+O(\chi^{-1}\log\chi)\right) \quad \text{as} \quad |\chi|\to\infty. \tag{2.16}$$

We can now relate the above asymptotic behaviour of $Z(\chi)$ to the flow (2.3) shown in figure 1. From (2.3) we find that in the main part of the fluid, as $|\chi|\to\infty$,

$$Z=\tfrac{1}{2}\mathrm{e}^{2\mathrm{i}\pi/3}(-3\mathrm{i}\chi)^{2/3}\left[1+O(\chi^{-1/3})\right]. \tag{2.17}$$

Hence,

$$\begin{aligned} h=\frac{Z-Z_0}{z-z_0} &= 2^{1/3}\mathrm{e}^{\mathrm{i}\pi/3}\left[1+O(\chi^{-1/3})\right] && \text{as} \quad |\chi|\to\infty;\\ &= 2^{1/3}\mathrm{e}^{\mathrm{i}\pi/3}\left[1+O((\Omega-1)^{1/3})\right] && \text{as} \quad \Omega\to1;\\ &= 2^{1/3}\mathrm{e}^{\mathrm{i}\pi/3}\left[1+O(\theta^{1/3})\right] && \text{as} \quad \theta\to0. \end{aligned} \tag{2.18}$$

An argument similar to the one above shows that in the jet region, as $\Omega\to-1$ and $\theta\to\pm\pi$:

$$h \;=\; 1+O(\chi^{-1/3}) \;=\; 1+O((\Omega+1)^{1/3}) \;=\; 1+O((\theta\mp\pi)^{2/3}). \tag{2.19}$$

Thus, h is continuous on ∂T, and has an absolutely convergent Fourier series with respect to θ. Hence the Faber polynomial series for $(Z-Z_0)/(z-z_0)$ should converge to a flow which resembles Stokes corner flow, with the free-surface streamlines asymptotic to straight lines inclined at $\pm30°$ to the horizontal. However, $\mathrm{d}h/\mathrm{d}\Omega=O((\Omega-1)^{-2/3})$ as $\Omega\to1$, so when it is expressed as a function of θ it has a singularity which is not square-integrable. This means that the expression for the fluid velocity contains a divergent series, and so does (2.8). In practice, the numerical solution method used in this paper nevertheless gave reasonable results when up to 128 terms were used in the series, corresponding to $\leqslant 256$ collocation points on the free surface.

2.5. *Uniqueness of the flow*

I have assumed that the flow is unique, given the position of the stagnation point S, and the flux Ψ which determines the length and velocity scales ($L=g^{-1/3}\Psi^{2/3}$, $V=(g\Psi)^{1/3}$). Trivial modifications include reflection in a vertical plane and reversal of the flow direction. I do not have a rigorous proof of uniqueness, but uniqueness is suggested by analogy with various other free-surface flows.

The 'almost-highest wave' inner solution of Longuet-Higgins & Fox (1977) depends on a single parameter, the velocity at the crest. Varying this velocity just changes the geometrical scale of the flow, as in the present case when Ψ is varied. The

present case of a breaking wave crest could be considered as an inner solution for a 'just-greater-than-highest' wave.

For a jet rising and falling under gravity, in the limiting case which has a 120° stagnation point at the crest (Vanden-Broeck & Keller 1982), the solution is determined by the flux in the jet, and varying the flux also just changes the scale. The same applies for the breaking wave in shallow water with a stagnation point at infinity, studied by Dias & Tuck (1993).

The flow past an inclined surfboard on the rear face of a solitary wave (Ting & Keller 1974; Vanden-Broeck & Keller 1989), which may have a jet thrown up at the leading edge of the board, appears to depend on three parameters: the flux in the jet, the angle of inclination of the board, and the length of the part of the board in contact with the fluid. If the flux in the jet is fixed, the number of free parameters is reduced to two, and if the length of the board is then reduced to zero, the inclination angle of the board must necessarily become zero since the surface must be horizontal at the stagnation point. The number of free parameters is thus reduced to zero, and the present breaking-crest flow should be reproduced in the limit as the bottom recedes to an infinite distance below the crest.

3. Conclusion

An approximate model for a breaking-wave crest has been presented, which assumes that the flow is incompressible, irrotational and steady. It neglects the interaction of the jet of the breaker with the fluid in the forward face of the wave. The flow is computed using conformal transformations, employing a Faber polynomial expansion in a transformed domain of finite extent, and applying the Bernoulli condition at a number of collocation points on the free surface. The resulting shape of the breaker is similar to those observed in laboratory experiments and time-dependent numerical computations at instants prior to the jet plunging through the interface. The maximum acceleration of $\approx 5.4g$ on the underside of the crest is in agreement with time-dependent computations (e.g. Dommermuth *et al.* 1988).

By analogy with some other free-surface flows, the solution appears to be unique if the flux Ψ through the jet is specified. Changing Ψ or the gravitational acceleration just alters the length and velocity scales of the flow. The solution may perhaps be regarded as a limiting case of the flow, with a jet, past a surfboard on the rear face of a solitary wave (Vanden-Broeck & Keller 1989).

The simple model presented here has been applied to the calculation of the wave energy dissipation due to breaking crests (Jenkins 1994). It can also be used in the calculation of forces on fixed and floating structures, mixing, the entrainment of air bubbles, particle deposition from the atmosphere, and so on. For calculating mixing and entrainment effects, it may be possible to consider the effect of the jet separately, and thus apply the results of laboratory experiments with artificial jets (e.g. Hwang *et al.* 1991).

The solution method which is employed here, using a Faber polynomial expansion in a non-circular domain, might be applied to other free-surface flow problems. As well as for jets, it could be used in the investigation of Rayleigh–Taylor instability (cf. Birkhoff & Carter 1956; Meiron, Orszag & Israeli 1981; Menikoff & Zemach 1983; Zemach 1986).

I would like to thank Howell Peregrine and three anonymous referees for constructive criticism which helped to improve the manuscript. The revised manuscript

was prepared at the Nansen Environmental and Remote Sensing Center, under the project 'Synthetic Aperture Radar Analysis and Modelling for Ocean Monitoring', funded by the Research Council of Norway.

REFERENCES

BERVI, N. 1894 On motion of a fluid with the formation of a surface of separation under the influence of gravity. *Proceedings of the Department of Physical Science of the Imperial Society of Natural Science, Moscow* 7, 49–56.

BIRKHOFF, G. & CARTER, D. 1956 Taylor instability. Appendices to report LA-1862. *Los Alamos Rep.* LA-1927.

BIRKHOFF, G. & ZARANTONELLO, E. H. 1957 *Jets, Wakes, and Cavities*. Academic.

BONMARIN, P. 1989 Geometric properties of deep-water breaking waves. *J. Fluid Mech.* **209**, 405–433.

CLARKE, N. S. 1965 On two-dimensional inviscid flow in a waterfall. *J. Fluid Mech.* **22**, 359–369.

DIAS, F. & CHRISTODOULIDES, P. 1991 Ideal jets falling under gravity. *Phys. Fluids* A **3**, 1711–1717.

DIAS, F., KELLER, J. B. & VANDEN-BROECK, J.-M. 1988 Flows over rectangular weirs. *Phys. Fluids* **31**, 2071–2076.

DIAS, F. & TUCK, E. O. 1993 A steady breaking wave. *Phys. Fluids* A **5**, 277–279.

DOLD, J. W. 1992 An efficient surface-integral algorithm applied to unsteady gravity waves. *J. Comput. Phys.* **103**, 90–115.

DOLD, J. W. & PEREGRINE, D. H. 1984 Steep unsteady waves: an efficient computational scheme. In *Nineteenth Coastal Engineering Conf.* (ed. B. L. Edge), pp. 955–967. American Society of Civil Engineers.

DOMMERMUTH, D. G., YUE, D. K. P., LIN, W. M., RAPP, R. J., CHAN, E. S. & MELVILLE, W. K. 1988 Deep-water plunging breakers: a comparison between potential theory and experiments. *J. Fluid Mech.* **189**, 423–442.

FENG, Z.-X. 1988 An alternative iteration algorithm for moving boundary free flow using boundary elements. In *Boundary Elements X* (ed. C. A. Brebbia), vol. 2, pp. 129–142. Computational Mechanics & Springer.

GEER, J. & KELLER, J. B. 1979 Slender streams. *J. Fluid Mech.* **93**, 97–115.

GOH, K. H. M. & TUCK, E. O. 1985 Thick waterfalls from horizontal slots. *J. Engng Maths* **19**, 341–349.

GREENHOW, M. 1983 Free-surface flows related to breaking waves. *J. Fluid Mech.* **134**, 259–275.

GUREVICH, M. I. 1966 *The Theory of Jets in an Ideal Fluid*. Pergamon.

HASSELMANN, K. 1974 On the spectral dissipation of ocean waves due to white capping. *Boundary-Layer Met.* **6**, 107–127.

HENRICI, P. 1986 *Applied and Computational Complex Analysis*, vol. 3. Wiley.

HWANG, P. A., POON, Y.-K. & WU, J. 1991 Temperature effects on generation and entrainment of bubbles induced by a water jet. *J. Phys. Oceanogr.* **21**, 1602–1605.

JENKINS, A. D. 1994 A quasi-stationary irrotational solution for a breaking wave crest. In *The Air-Sea Interface* (ed. M. Donelan, W. H. Hui & W. Plant). The University of Toronto Press.

JOHN, F. 1953 Two-dimensional potential flows with a free boundary. *Communs Pure Appl. Maths* **6**, 497–503.

KELLER, J. B. & GEER, J. 1973 Flows of thin streams with free boundaries. *J. Fluid Mech.* **59**, 417–432.

LEE, J. & VANDEN-BROECK, J.-M. 1993 Two-dimensional jets falling from funnels and nozzles. *Phys. Fluids* A **5**, 2454–2460.

LONGUET-HIGGINS, M. S. 1976 Self-similar, time-dependent flows with a free surface. *J. Fluid Mech.* **73**, 603–620.

LONGUET-HIGGINS, M. S. 1980*a* A technique for time-dependent, free-surface flows. *Proc. R. Soc. Lond.* A **371**, 441–451.

LONGUET-HIGGINS, M. S. 1980*b* On the forming of sharp corners at a free surface. *Proc. R. Soc. Lond.* A **371**, 453–478.

LONGUET-HIGGINS, M. S. 1981 On the overturning of gravity waves. *Proc. R. Soc. Lond.* A **376**, 377–400.

LONGUET-HIGGINS, M. S. 1982 Parametric solutions for breaking waves. *J. Fluid Mech.* **121**, 403–424.

LONGUET-HIGGINS, M. S. 1983 Rotating hyperbolic flow: particle trajectories and parametric representation. *Q. J. Mech. Appl. Maths* **36**, 247–270.

LONGUET-HIGGINS, M. S. & COKELET, E. D. 1976 The deformation of steep surface waves on water. I. A numerical method of computation. *Proc. R. Soc. Lond.* A **350**, 1–26.

LONGUET-HIGGINS, M. S. & FOX, M. J. H. 1977 Theory of the almost-highest wave: the inner solution. *J. Fluid Mech.* **80**, 721–741.

MEIRON, D. I., ORSZAG, S. A. & ISRAELI, M. 1981 Applications of numerical conformal mapping. *J. Comput. Phys.* **40**, 345–360.

MENIKOFF, R. & ZEMACH, C. 1983 Rayleigh–Taylor instability and the use of conformal maps for ideal fluid flows. *J. Comput. Phys.* **51**, 28–64.

MILLER, R. L. 1957 Role of vortices in surf zone prediction: sedimentation and wave forces. In *Beach and Nearshore Sedimentation* (ed. R. A. Davis & R. L. Ethington), pp. 92–114. Society of Economic Palaeontologists and Mineralogists.

NAG 1990 *The NAG Fortran Library Manual, Mark 14.* Numerical Algorithms Group.

NEW, A. L. 1983 A class of elliptical free-surface flows. *J. Fluid Mech.* **130**, 219–239.

NEW, A. L., MCIVER, P. & PEREGRINE, D. H. 1985 Computations of overturning waves. *J. Fluid Mech.* **150**, 233–251.

SAWADA, H. & TOMITA, H. 1994 On the dynamical properties of plunging breakers in deep water. In *The Air-Sea Interface* (ed. M. Donelan, W. H. Hui & W. Plant). The University of Toronto Press.

SEO, S. N. & DALRYMPLE, R. A. 1990 An efficient model for periodic overturning waves. *Engineering Analysis with Boundary Elements* **7**, 196–204.

TING, L. & KELLER, J. B. 1974 Planing of a flat plate at high Froude number. *Phys. Fluids* **17**, 1080–1086.

TUCK, E. O. 1987 Efflux from a slit in a vertical wall. *J. Fluid Mech.* **176**, 253–264.

VANDEN-BROECK, J.-M. & KELLER, J. B. 1982 Jets rising and falling under gravity. *J. Fluid Mech.* **124**, 335–345.

VANDEN-BROECK, J.-M. & KELLER, J. B. 1986 Pouring flows. *Phys. Fluids* **29**, 3958–3961.

VANDEN-BROECK, J.-M. & KELLER, J. B. 1989 Surfing on solitary waves. *J. Fluid Mech.* **198**, 115–125.

VINJE, T. & BREVIG, P. 1981 Breaking waves on finite water depths: a numerical study. *Ship Res. Inst. of Norway, Rep.* R-111.81.

WEGMANN, R. 1978 An iterative method for conformal mapping. *Numer. Math.* **30**, 453–466. (English translation: 1986 *J. Comput. & Appl. Math.* **14**, 7–18.)

ZEMACH, C. 1986 A conformal map formula for difficult cases. *J. Comput. & Appl. Math.* **14**, 207–215.